SIMULATION STUDY INTO THE DETECTION OF LOW- AND HIGH-Z MATERIALS IN CARGO CONTAINERS USING COSMIC RAY MUONS*

Anzori Sh. Georgadze

Institute for Nuclear Research of National Academy of Sciences of Ukraine
Kyiv, Ukraine
and
Institute of Physics, University of Tartu, Estonia

Received 24 November 2023, accepted 2 January 2024,
published online 26 February 2024

Cosmic ray muon scattering tomography is a non-invasive screening technique that can provide three-dimensional images of the internal structure of large objects such as shipping containers, allowing for comprehensive searches for hidden illicit items. Cosmic ray muons possess substantially higher energies compared to typical X-rays, which gives them the ability to penetrate large and dense materials. This unique characteristic makes muon scattering tomography a valuable tool for identifying materials hidden inside shielding that may be too thick or deep for other imaging methods such as X-rays or conventional gamma-ray scanning. We report a Geant4 simulation study for the detection of low- and high-Z illicit objects hidden inside a legal cargo in a shipping container. We have used the Point of Closest Approach (PoCA) reconstruction algorithm to create the three-dimensional image of a shipping container and have applied image processing tools to improve signal-to-noise ratio for detection of illicit objects inside the legal cargo. Simulation and reconstruction results showed that the applied method can detect illicit materials within a minute time scale.

DOI:10.5506/APhysPolBSupp.17.1-A2

1. Introduction

Every year, several hundreds of millions of shipping containers pass through the container terminals of the harbors all over the world. Containers have become a fundamental element of the modern logistics and transportation industry, revolutionizing the way goods are transported and facilitating efficient and secure global trade. At present, a majority of EU

* Presented at the Symposium on *New Trends in Nuclear and Medical Physics*, Kraków, Poland, 18–20 October, 2023.

ports have scanning devices on their premises, mainly used to scan imported containers. The share of containers scanned ranges from 0.1% in bigger ports to 3% in smaller ones [1]. The cargo imaging inspection systems are aimed at finding illegal Hazardous or Dangerous (HoD) materials, such as weapons, explosives, drugs or Special Nuclear Materials (SNM) through the imaging of cargo containers and trucks. Conventional X-ray techniques are often used for container scanning in border control and customs applications. X-ray systems introduce ionizing radiation, which can be hazardous to human health, therefore, such imaging systems require shielding. Fully passive muon tomography is a promising alternative or a complementary approach to the standard radiographic techniques for scanning shipping containers as a non-invasive and non-destructive means of detecting potential threats or contraband [2]. The technique relies on the natural occurrence of cosmic ray muons, which are highly penetrating particles [1, 2] and, therefore, does not introduce additional levels of ionizing radiation. At sea level, the muon rate is about 10,000 per minute per square meter [2] and their energy distribution is peaked at 3–4 GeV. Due to the dependence of the scattering angle on the atomic number Z of the material, this technique is considered promising to prevent smuggling of the Special Nuclear Materials [3] but also is studied for detection of explosives and drugs [4–6].

In this paper, we report on the results of using Monte Carlo simulations to evaluate the performance of muon tomography systems for detecting HoD low- and high-Z materials in cargo containers.

2. Geant4 simulation and tomographic reconstruction

Simulation model of the muon tomography system consisting of two tracking modules above and below the shipping container was constructed with the Geant4 toolkit [7]. Each tracking module, having two position-sensitive detectors, was modeled as a plane of plastic scintillators with a detection efficiency of 100%, an area of 8 m $\times$ 4 m, and fit that of a shipping container.

As a possible tracking detector concept we consider technology based on plastic scintillating fiber arrays readout with Silicon Photomultipliers (SiPMs) [8]. The tracker consists of two planes, with the two layers of fibers in each plane oriented perpendicularly to those in the adjacent plane, which allow for three-dimensional reconstruction of the muon track (Fig. 1). The Cosmic-Ray Shower Library (CRY) [9] was used to generate muons for the latitude 50° and altitude at sea level. The origin points of generated muons were sampled from a horizontal plane surface of 10 m $\times$ 10 m. Generated muons are interfaced with Geant4 to simulate the interaction of the muons with the detector, shipping container, and cargo. We use the standard physics list for high-energy transport named “FTFP_BERT”.

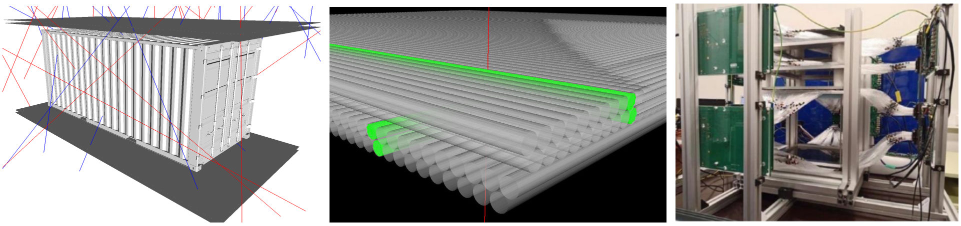

(a) (b) (c)

Fig. 1. (a) Layout of the plastic scintillator fiber tracker in Geant4 with optical photons generated in fibers by muon; (b) plastic scintillator fiber tracker with an area 30×30 cm^2 constructed in [8].

Cosmic ray muon scattering tomography is achieved by tracking the trajectories of both incoming and outgoing muons using a set of position-sensitive detectors. The recorded data on the hit position on each detector layer are used to produce two tracks. We calculate the scattering angle between the trajectories of incoming ($\vec{v}_1$) and outgoing ($\vec{v}_2$) muons using formula [10]

$$\theta_{\mathrm{scatt}} = \arccos\left(\frac{\vec{v}_1 \cdot \vec{v}_2}{|v_1|\,|v_2|}\right) .$$

For the reconstruction of tomographic images we have used the Point-of-Closest-Approach algorithm (PoCA) [11], which is based on the assumption that muon scattering occurs in a single point. In order to take into account detector position resolution we reconstruct the PoCA points with hit positions in the tracking detector smeared simultaneously in X and Y directions by Gaussian with the resolution σ of 0.15 mm obtained in [8]. Synthetic datasets were analyzed using the ROOT data analysis package [12].

To simulate realistic smuggling scenarios, we developed a detailed model of a shipping container ($609.6 \times 259.1 \times 243.8$ cm^3) in Geant4 with legal goods in cardboard boxes on standard pallets (Fig. 2). The HoD material — RDX was hidden among boxes of legal goods, in each of the 10 pallets, one randomly selected box is loaded with RDX (density 1.812 g/cm^3). We simulated three scenarios with cloths (density 0.2 g/cm^3), bananas (0.4 g/cm^3), and dry pasta (1.0 g/cm^3). The densities of legal materials were calculated based on wholesale market data. The simulated data samples were produced with an exposure time of 10 minutes (10 million muons).

The other simulated scenarios are the concealment of SNM in a shipping container under various conditions, such as a full load of dry pasta or in the engine compartment of a sports car being transported inside the container. The simulated time for these scenarios was 5 minutes.

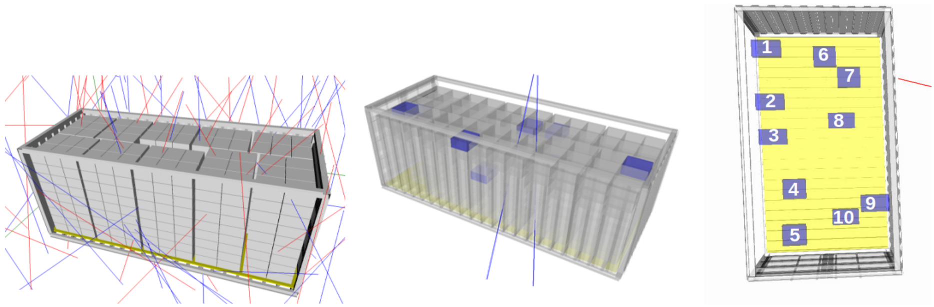

(a) (b) (c)

Fig. 2. (a) Visualization of tomography station with a shipping container in Geant4; (b) shipping container loaded with card boxes on standard pallets; (c) visualization of positioning of boxes with RDX in the cargo container.

3. Image processing

Since some of the hits create statistical noise, several selection criteria were implemented to select only relevant scattering points. As the dimensions of the container are known, the outer voxels can be removed trough a cube shape spatial cut on the image to dimensions $585 \times 235 \times 235$ cm^3 which correspond to the internal part of the container. We apply the scattering angle cut which is set to 10 milliradians for an analysis of low-Z HoD materials and 100 milliradians for searching for SNM.

Since the cosmic muon flux is relatively weak, the small population of reconstructed scattering centers in voxel leads to large fluctuations in the number of scattering points. To mitigate this effect, we apply a statistical filtering method by finding a median value among the 26 nearest neighbor voxels (Fig. 3 (a)) and assigning this value to a given voxel. This constitutes the image smoothing using the first nearest neighbor data. In the case of

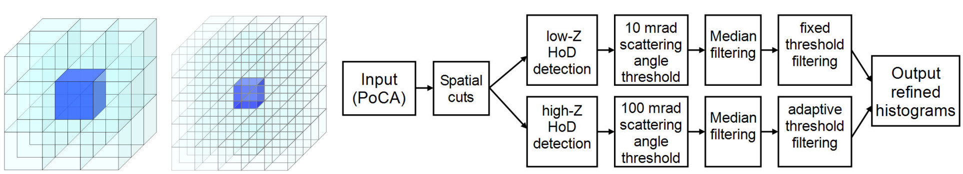

(a) (b) (c)

Fig. 3. (a) Illustration of the nearest neighbor technique considering the first layer around a given voxel; (b) the second nearest neighbor layer can be used to improve data smoothing for muon tomography image processing; (c) schematic diagram of the algorithms applied for image processing and analysis.

inhomogeneous distribution of scattering density, we calculate the median value over two nearest neighbor layers of a given voxel, which accounts for 80 voxels (Fig. 3 (b)). The nearest neighbor filtering method removes noise by replacing the value of a voxel at a given location with the median value in its immediate neighborhood. This smoothing method helps to effectively identify concentrated points when the average value is taken over a homogeneous area.

HoD material can be detected by the difference in scattering density of HoD and legal material. To do that, the nearest neighbor voxel values are compared to a threshold value. If a number of reconstructed PoCA points weighted with the scattering angle in the voxel lower than a fixed threshold, then the voxel value is set to 0. Fixed threshold filtering technology works well to remove the background from the clutter of a legal cargo consisting of low-Z materials. When the cargo is composed of low- and medium-Z materials, they create a non-uniform scattering density distribution, so fixed threshold filtering for background removal becomes ineffective. To cope with the heterogeneous background, we use an adaptive threshold algorithm based on a function that estimates the distribution of the far-scattering density. The adaptive thresholding algorithm determines the threshold for a voxel based on up to ten neighboring layers around a given voxel. This algorithm is particularly effective at removing mixed background from low- to mid-Z materials such as concrete, aluminum, steel, and copper, as well as aggregating voxels containing high scattering density weighted by the scattering angle, which resulted from the presence of high-Z material. This algorithm is mainly used to search for smuggled SNM in a cargo container. A schematic diagram of the tomographic image analysis process is presented in Fig. 3 (c).

4. Results

Reconstructed and analyzed according to the previously described procedure tomographic images for the scenario of RDX inside cargo are shown in Figs. 4 and 5. Boxes of RDX are easy to distinguish among cloths and bananas. Detection of RDX in dry pasta in 3D tomographic imaging is questionable therefore we segmented the tomographic image into four horizontal slices 50 cm thick (Fig. 5) and examined their XY projections. On these slices, all ten boxes of RDX are visualized. Figure 4 (d) shows for comparison the radiographic image of the scenario of boxes of RDX hidden in dry pasta simulated with Geant4 using an energy spectrum of 9 MeV X-rays. As can be seen, muon tomography has the advantage of being able to create a three-dimensional tomographic image.

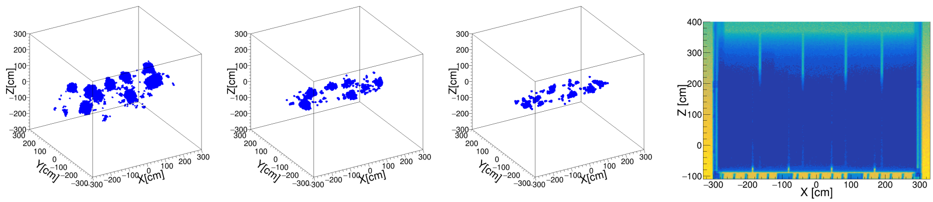

(a) (b) (c) (d)

Fig. 4. (a) Reconstructed muon tomographic images for the scenario of RDX hidden in container among cloths; (b) muon tomographic images of RDX in bananas and (c) in dry pasta; (d) X-ray radiographic image simulated in Geant4 for the scenario of boxes of RDX hidden in dry pasta.

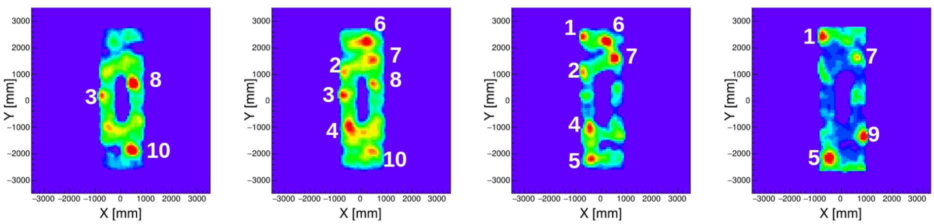

(a) (b) (c) (d)

Fig. 5. Tomographic reconstruction of the RDX hidden in dry pasta scenario for four 50 cm slices in the XY plane centered at $Z = -750$ cm (a), $Z = -250$ cm (b), $Z = 250$ cm (c), and $Z = 750$ cm (d). Bright red spots on XY slices indicate the presence of high-density material. Since the vertical muon flux is several times greater than the lateral muon flux, the reconstructed RDX boxes are longer in the Z direction and are therefore visible in other slices.

Figure 6 (a) shows 10 SNM cubes, each measuring 10 cm^3, hidden inside boxes of dry pasta, Fig. 6 (b) shows the reconstructed tomographic image after applying the scattering angle cut and median filtering, and Fig. 6 (c) demonstrates further image processing using the adaptive threshold filtering method. The adaptive threshold filtering method completely suppresses noise from the cargo, allowing to detect all ten SNM cubes.

Figure 7 shows a sports car inside a container with a hidden SNM. Its tomographic images are shown after applying median filtering Fig. 7 (b) and after applying the adaptive threshold filtering method Fig. 7 (c). It can be seen that in this scenario, a 10 cm^3 SMN is successfully identified, and the noise from the container, engine, and car body are almost completely reduced.

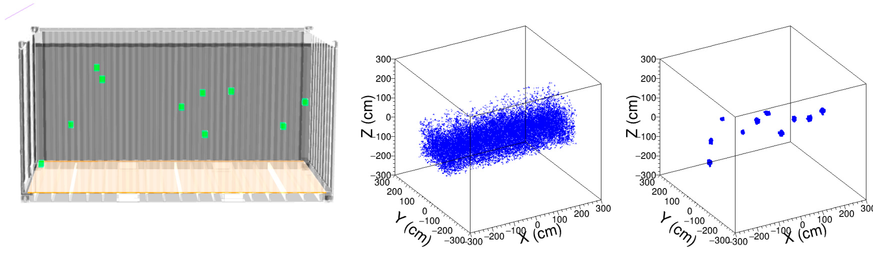

(a) (b)

Fig. 6. (a) Geant4 visualization of the scenario of 10 cubes of SNM hidden inside dry pasta; (b) tomographic reconstruction after mean filtering applied; (c) tomographic reconstruction using the adaptive threshold algorithm. For visualization purposes, carton boxes are made invisible.

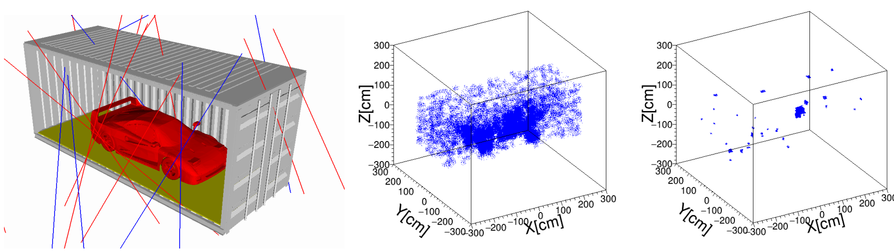

(a) (b) (c)

Fig. 7. (a) Simulated in the Geant4 scenario with a sports car inside the container and SNM inside the car; (b) tomographic reconstruction after mean filtering and the scattering angle cut applied; (c) tomographic reconstruction using the adaptive threshold algorithm. SNM with a volume of 10 cm^3 is clearly visible.

5. Conclusions

In this work, different smuggling scenarios of low- and high-Z HoD materials were investigated through Monte Carlo simulations. We tested the performance of the image processing tools on both low- and high-Z materials using PoCA reconstruction. The algorithms used are fast and suitable for the real-time processing of tomographic images. They allow for efficient background removal from cargo materials, making detection of HoD materials possible. The developed adaptive threshold filtering algorithm is critical for effective background removal. The idea of dynamically setting thresholds accounts for the variations in scattering density observed across different layers. This adaptability ensures that the algorithm will respond to changes in density patterns, providing more accurate identification of both low- and high-Z materials.

Simulation and data analysis results show that muon tomography is a promising method for combating the smuggling of hazardous or dangerous materials using shipping containers.

REFERENCES

[1] «Secure Trade and 100% scanning of containers», Technical report, European Commission Staff Working Paper, 2010.

[2] S. Barnes *et al.*, *Instruments* **7**, 13 (2023).

[3] K.N. Borozdin *et al.*, *Nature* **422**, 277 (2003).

[4] L. Cuéllar *et al.*, «Soft cosmic ray tomography for detection of explosives», *IEEE Nuclear Science Symposium Conference Record (NSS/MIC)*, 2009, pp. 968–970.

[5] Z. Yifan *et al.*, *High Power Laser and Particle Beams* **30**, 086002 (2018).

[6] J. Chen *et al.*, *J. Instrum.* **18**, P08008 (2023).

[7] S. Agostinelli *et al.*, *Nucl. Instrum. Methods Phys. Res. A* **506**, 250 (2003).

[8] G. Anbarjafari *et al.*, arXiv:2102.12542 [physics.ins-det].

[9] C. Hagmann, D. Lange, D. Wright, «Cosmic-ray shower generator (CRY) for Monte Carlo transport codes», *IEEE Nuclear Science Symposium Conference Record*, 2007, pp. 1143–1146.

[10] T. Carlisle, J. Cobb, D. Neuffer, «Multiple scattering measurements in the MICE experiment», *Proceedings of IPAC2012*, New Orleans, Louisiana, USA, 2012, pp. 1419–1421.

[11] S. Riggi *et al.*, *Nucl. Instrum. Methods Phys. Res. A* **728**, 59 (2013).

[12] I. Antcheva *et al.*, *Comput. Phys. Commun.* **180**, 2499 (2009).